

Melting of $c\bar{c}$ and $b\bar{b}$ pairs in the pre-equilibrium stage of proton-nucleus collisions at the Large Hadron Collider

Lucia Oliva,^{1,2,*} Gabriele Parisi,^{1,3,†} and Marco Ruggieri^{1,2,‡}

¹*Department of Physics and Astronomy "Ettore Majorana",*

University of Catania, Via Santa Sofia 64, I-95123 Catania, Italy

²*INFN-Sezione di Catania, Via Santa Sofia 64, I-95123 Catania, Italy*

³*INFN-Laboratori Nazionali del Sud, Via Santa Sofia 62, I-95123 Catania, Italy*

We study the melting of $c\bar{c}$ and $b\bar{b}$ pairs in the early stage of high-energy proton-nucleus collisions. We describe the early stage in terms of an evolving $SU(3)$ glasma stage, that is dominated by intense, out-of-equilibrium gluon fields. On top of these fields, we liberate heavy quark-antiquark pairs, whose constituents are let evolve according to relativistic kinetic theory coupled to the gluon fields. We define a pair-by-pair probability that the pair melts during the evolution, which we relate to the relative distance between the two particles in the pair, as well as to the fluctuations of the color charges induced by the interaction of the quarks with the gluon fields. We find that the fluctuations of the color charges favor the melting of the pairs. Moreover, we estimate that within 0.2 fm/c of proper time, measured with respect to the formation time of the pairs, about the 50% of $c\bar{c}$ and $b\bar{b}$ pairs melt as a result of the diffusion of the heavy quarks in the gluon fields; this time estimate doubles when color fluctuations are neglected.

PACS numbers: 12.38.Aw,12.38.Mh

Keywords: heavy quarks, glasma, proton-nucleus collisions

I. INTRODUCTION

Relativistic heavy-ion collisions, as performed at the Relativistic Heavy Ion Collider (RHIC) at Brookhaven National Laboratory and at the Large Hadron Collider (LHC) at CERN, provide a unique opportunity to investigate Quantum Chromodynamics (QCD) at extreme temperatures and densities. Over the past few decades, many experimental results indicated the emergence of a new state of matter, referred to as the Quark-Gluon Plasma (QGP), which forms within ~ 1 fm/c after the collision and in which quarks and gluons behave as a hydrodynamic fluid [1]. Such facilities are able to perform measurements also in smaller collision systems such as proton-proton (pp) and proton-nucleus (pA) [2, 3], and these have shown very similar features as those found in heavy ion collisions. While calculations within the hydrodynamic framework have been quite successful in describing observables in these small collision systems, the applicability of hydrodynamics becomes increasingly doubtful as the system size decreases and gradients increase [4, 5]. It is likely that both initial intrinsic momentum correlations and a hydro-like anisotropic expansion are necessary to understand the elliptic anisotropic emission in pA [6–11].

For this reason, a thorough treatment of the initial stages is even more important for pA collisions, and the Classical Yang-Mills (CYM) theory offers a good framework for the study of this stage. In fact, CYM well describes the out-of-equilibrium evolution of the highly

occupied gluonic system, named the glasma [12], that serves as the initial condition for the system produced in the collisions. The glasma is based on the Color-Glass-Condensate (CGC) effective theory, which stands as a valid description of high-energy nuclei [13–15], see [16–19] for reviews. The glasma initial condition has been widely used to establish the initial conditions for the subsequent hydrodynamic evolution [20, 21].

Heavy Quarks (HQs), i.e. charm, c , and beauty, b , represent a unique probe of the early stage of high-energy collisions as well as of the transport properties of the thermalized medium subsequently produced [22–62]. Indeed, due to the large masses, the HQs have a very short formation time of the order of 0.1 fm/c. Moreover, they have a thermalization time in the QGP medium which is comparable or larger than the entire lifetime of the QGP. Therefore, the HQ final states, the heavy-flavored hadrons, maintain imprint of the evolution dynamics during the whole collision evolution, with traces from both the initial stage and the subsequent QGP phase. Besides studies on the diffusion of HQs in the QGP and on their hadronization in relativistic nuclear collisions, several works have investigated the impact of the early stage on heavy quarks [63–81]. These have shown that heavy quarks undergo significant diffusion in the early stage, suggesting an impact on experimental observables such as the nuclear modification factor and the elliptic flow, as analysed in [65]. Since for small systems the thermalized QGP stage is short lived or even absent, HQs could keep a cleaner trace of the early stage with respect to nucleus-nucleus reactions. Thus, for pA collisions the impact of the initial glasma state on final heavy-quark observables may be predominant in the whole evolution of the collision event.

A natural extension of the aforementioned works is to

* lucia.oliva@dfa.unict.it

† gabriele.parisi@dfa.unict.it

‡ marco.ruggieri@dfa.unict.it

look at the impact of the gluon-dominated initial state on the evolution and dissociation of heavy quarkonia, which are bound states of heavy quarks and antiquarks of the same flavour, namely charmonium $c\bar{c}$ and bottomonium $b\bar{b}$. The production and suppression of heavy quarkonium states in hadronic collisions and in particular in QGP has been widely studied for almost four decades [33, 82–102]. In particular, the melting emerges from the interplay of several mechanisms, coming from the different phases of the collision, from initial HQ pair production through the QGP stage to final hadronization, see Ref. [103] for a review. As in the QGP, $c\bar{c}$ and $b\bar{b}$ pairs can dissociate in the evolving glasma as well, see [104], with important implications for their evolution in the ensuing QGP medium and for the determination of the heavy-flavoured final states produced at hadronization (both open heavy-flavour hadrons, such as D and B mesons, and regenerated quarkonia). In the evolving glasma, it is the HQ interaction with the classical color fields that leads to a modification of their spatial and momentum coordinates as well as of their color charge, thus affecting the probability that they survive to the pre-equilibrium stage and enter into the possibly-formed QGP phase as a pair.

In this article, we investigate the melting of $c\bar{c}$ and $b\bar{b}$ pairs during the pre-equilibrium stage of high-energy pA collisions, the latter being modeled within the glasma framework. The primary objective of this work is to determine the fraction of pairs that dissociate during the propagation in the evolving glasma, aiming also at disentangling the role of color-charge de-correlation of the HQ pair in the melting, which was only partly addressed before. Within our model the HQs in each pair, formed at $\tau = \tau_{\text{form}}$, couple to the strong gluon fields via Wong equations [105, 106] as it has been done in [104]. With respect to the approach presented in [104], we implement a different criterion for the calculation of the number of melting pairs, based on a survival probability, $\mathcal{P}_{\text{survival}}$, that takes into account both the spreading of the quark, Q , and its companion antiquark, \bar{Q} , in coordinate space, as well as the de-correlation of the color charges induced by the interactions of Q and \bar{Q} with the gluon fields in the early stage. $\mathcal{P}_{\text{survival}}$ is built similarly to the hadronization probability introduced in coalescence models [107–112]. We are able to estimate an average melting time for both $c\bar{c}$ and $b\bar{b}$ pairs, that turns out to be around 0.2 fm/c when fluctuations of the color charges are included in $\mathcal{P}_{\text{survival}}$, and that can be even twice larger when the fluctuations of the color charges are not taken into account in $\mathcal{P}_{\text{survival}}$. Differently from [104], we consider $N_c = 3$ and an initialization for pA collisions, that takes into account the event-by-event fluctuations of the color charges in the proton as well as in the initial distribution of the heavy quarks in the transverse plane. Moreover, within our model we allow for the expansion both along the longitudinal direction and in the transverse plane, while in [104] only a static geometry was considered.

Throughout this article we use natural units $k_B = c = \hbar = 1$. Moreover, we formulate the $SU(3)$ Yang-Mills

equations using the Milne coordinates

$$\tau = \sqrt{t^2 - z^2}, \quad \eta = \frac{1}{2} \ln \left(\frac{t+z}{t-z} \right), \quad (1)$$

where τ is the proper time and η denotes the space-time rapidity.

II. THE EVOLVING GLASMA IN PROTON-NUCLEUS COLLISIONS

A. Color charges for p and A

The CGC effective theory [13–15] is based on a separation of scales between the high Bjorken- x degrees of freedom, i.e. the valence partons, and the low x degrees of freedom which they generate, that is, soft gluons. To realize this separation, the sources of the initial gluon fields are generated using the McLerran-Venugopalan (MV) model, in which the large- x color sources are randomly distributed on an infinitely thin color sheet. The distribution of these charges is a Gaussian, characterized by zero average

$$\langle \rho^a(\mathbf{x}_\perp) \rangle = 0, \quad (2)$$

and variance given by

$$\langle \rho^a(\mathbf{x}_\perp) \rho^b(\mathbf{y}_\perp) \rangle = g^2 \mu^2 \delta^{ab} \delta^{(2)}(\mathbf{x}_\perp - \mathbf{y}_\perp). \quad (3)$$

Here, g is the coupling constant (we use $g = 2$, corresponding to $\alpha_s = 0.3$), and μ is the so-called MV parameter, describing the number density of the color charges per unit of area in the transverse plane. In our implementation, we relax the single-sheet hypothesis of the original MV model by generating a certain number N_s of color sheets stacked on top of one another [113]. Consequently, for each of the sheets, the numerical implementation of Eq. (3) we will use in this work is

$$\langle \rho_{n,x}^a \rho_{m,y}^b \rangle = g^2 \mu^2 \frac{\delta_{n,m}}{N_s} \delta^{a,b} \frac{\delta_{x,y}}{a_\perp^2}, \quad (4)$$

where $a, b = 1, \dots, N_c^2 - 1$ are $SU(3)$ color indexes, $n, m = 1, \dots, N_s$ are the color sheet indexes and x, y span each point of a $N_\perp \times N_\perp$ lattice, whose transverse length is L_\perp and lattice spacing is $a_\perp = L_\perp / N_\perp$. Operatively, conditions (2) and (4) are satisfied by generating random Gaussian numbers with mean zero and standard deviation equal to $\sqrt{(g^2 \mu^2) / (N_s a_\perp^2)}$. Below we explain how to build up the gluon fields generated by each sheet, and how to combine all these fields to obtain the initial gluon field in the glasma. Unless otherwise stated, we use $N_s = 50$ in Eq. (4), having checked that this number of sheets is enough to get numerical convergence.

These steps are shared by the charge generation of both a proton and a heavy ion. Indeed, the original MV model assumed a source charge density that was homogeneous

in the transverse plane, which is feasible when dealing with large-A nuclei, whose details at the level of single nucleons can be neglected. On the other hand, a reasonable description of protons involves a varying nuclear density in the transverse plane to take into account the underlying quark structure. The main difference between those two cases lies in the choice of μ : in the A-case μ is chosen as a constant equal to $\mu = 0.5$ GeV, which translates into uniform fluctuations of color charge throughout the lattice. The p-case is instead more involved. In order to do so, let us introduce the thickness function of the proton T_p , normalized to 1 and defined as

$$T_p(\mathbf{x}_\perp) = \frac{1}{3} \sum_{i=1}^3 \frac{1}{2\pi B_q} \exp\left(-\frac{(\mathbf{x}_\perp - \mathbf{x}_i)^2}{2B_q}\right), \quad (5)$$

where the \mathbf{x}_i denote the positions of the constituent quarks, which are randomly extracted from the distribution

$$T_{cq}(\mathbf{x}_\perp) = \frac{1}{2\pi B_{cq}} \exp\left(-\frac{\mathbf{x}_\perp^2}{2B_{cq}}\right). \quad (6)$$

Parameters have been chosen as $B_q = 0.3$ GeV⁻², $B_{cq} = 4$ GeV⁻², i.e. the widths of the two Gaussians differ by a factor around 4. After doing so, we evaluate the saturation scale Q_s in this model as

$$Q_s^2(x, \mathbf{x}_\perp) = \frac{2\pi^2}{N_c} \alpha_s \cdot xg(x, Q_0^2) \cdot T_p(\mathbf{x}_\perp). \quad (7)$$

from which $\mu(x, \mathbf{x}_\perp)$ is given by [114]

$$g^2\mu(x, \mathbf{x}_\perp) = cQ_s(x, \mathbf{x}_\perp), \quad (8)$$

with $c = 1.25$. Note that by virtue of Eq. (7) not only μ , but also Q_s depend on the transverse plane coordinates. Also, in principle xg in (7) should be computed at the scale Q_s by means of the DGLAP equation with a proper initialization. This was done in [114, 115], and we reserve this approach for future studies. For the sake of simplicity, in the present study we limit ourselves by assuming that xg is given by the initial condition at $Q_0^2 = 1.51$ GeV² as in [114, 115], namely

$$xg(x, Q_0^2) = A_g x^{-\lambda_g} (1-x)^{f_g}, \quad (9)$$

with $A_g = 2.308$, $\lambda_g = 0.058$ and $f_g = 5.6$. This simplification is partly justified by the fact that the average saturation scale for the proton is of the order of $Q_s \sim 1$ GeV, hence we do not expect the DGLAP evolution of the xg in Eq. (9) to lead to significant changes. For pA collisions at the LHC energy, the relevant values of x are in the range $[10^{-4}, 10^{-3}]$. In our calculations, we will thus fix x in the aforementioned range, then compute xg by virtue of Eq. (9). If not stated otherwise, we will use the corresponding value obtained for $x = 10^{-4}$, that is, $xg = 3.94$.

B. Gauge-link formulation of the evolving glasma

Once the charge has been generated, we know that the hard and the soft sectors are coupled via the Yang-Mills equations [116]

$$D_\mu F^{\mu\nu} = J^\nu, \quad (10)$$

where $D_\mu = \partial_\mu - ig[A_\mu, \cdot]$ is the covariant derivative, $F^{\mu\nu} = \partial^\mu A^\nu - \partial^\nu A^\mu - ig[A^\mu, A^\nu]$ is the field strength tensor and J^μ the color current. Using the light-cone coordinates, the conservation of current implies $A^- = 0$. Moreover, by working in the covariant gauge we can also impose $A^i = 0$, where $i = x, y$. The only component left is therefore $A^+ \equiv \alpha$, which can be seen to obey the following Poisson equation

$$\Delta_\perp \alpha(\mathbf{x}_\perp) = -\rho(\mathbf{x}_\perp). \quad (11)$$

In order to solve this equation, we introduce a soft regulator, m , then Fourier-transform both sides of (11), getting

$$\tilde{\alpha}_{n,k}^a = \frac{\tilde{\rho}_{n,k}^a}{\tilde{k}_\perp^2 + m^2}, \quad (12)$$

where the discretized momentum \tilde{k}_\perp is given by

$$\tilde{k}_\perp^2 = \sum_{i=x,y} \left(\frac{2}{a_\perp}\right)^2 \sin^2\left(\frac{k_i a_\perp}{2}\right), \quad (13)$$

and $m = 0.2$ GeV = 1 fm⁻¹, which acts as a screening mass and effectively implements color confinement on lengths above $1/m$. By then, Fourier-transforming back, we get $\alpha(\mathbf{x}_\perp)$ in coordinate space.

Once we obtained a solution for the gauge field in the covariant gauge, the Wilson line for each nucleus is evaluated as

$$V_{\mathbf{x}} = \prod_{n=1}^{N_s} \exp\{ig\alpha_{n,\mathbf{x}}^a t^a\} \quad (14)$$

and then obtain the gauge links, U , for each of the two nuclei as

$$U_{\mathbf{x},i}^{A,B} = V_{\mathbf{x}}^{A,B} V_{\mathbf{x}+\hat{i}}^{\dagger,A,B}. \quad (15)$$

In the above expressions t^a are the $SU(3)$ group generators, i.e. the eight Gell-Mann matrices divided by 2. If the point \mathbf{x}_\perp belongs to the edge of the simulation lattice, periodic boundary conditions have been implemented.

The gauge link resulting from the interaction of the two colored glasses in p and A, $U_{\mathbf{x},i}$, at the position \mathbf{x} in the transverse plane is determined by solving a set of eight equations, which are

$$\text{Tr}[t_a(U_{\mathbf{x},i}^A + U_{\mathbf{x},i}^B)(\mathbb{I} + U_{\mathbf{x},i}) - \text{h.c.}] = 0, \quad (16)$$

with $a = 1, \dots, N_c^2 - 1$. In the case of $N_c = 2$ there is an exact solution of (16) for $U_{\mathbf{x},i}$ [117]. Instead, for

$SU(3)$ we can solve (16) only numerically via a standard iterative method. Using this procedure we calculate the gauge links along the x and y direction. For the longi-

tudinal components we initialize simply $U_\eta = \mathbb{I}$ since the glasma has $A_\eta = 0$ at $\tau = 0^+$. The initial color-electric fields are [118]

$$E_x = E_y = 0,$$

$$E^\eta = -\frac{i}{4ga_\perp^2} \sum_{i=x,y} \left[(U_i(\mathbf{x}_\perp) - \mathbb{I})(U_i^{B,\dagger}(\mathbf{x}_\perp) - U_i^{A,\dagger}(\mathbf{x}_\perp)) + (U_i^\dagger(\mathbf{x}_\perp - \hat{i}) - \mathbb{I})(U_i^{B,\dagger}(\mathbf{x}_\perp - \hat{i}) - U_i^{A,\dagger}(\mathbf{x}_\perp - \hat{i})) - h.c. \right]. \quad (17)$$

After the initial condition has been fixed, The equations of motion for the gauge links are [118]

$$\partial_\tau U_i(\mathbf{x}) = \frac{-iga_\perp}{\tau} E^i(\mathbf{x}) U_i(\mathbf{x}), \quad (18)$$

$$\partial_\tau U_\eta(\mathbf{x}) = -iga_\eta \tau E^\eta(\mathbf{x}) U_\eta(\mathbf{x}), \quad (19)$$

where a_η denotes the discretization step in the η direction. In order to reduce the discretization error in time, we drive the evolution through a leapfrog algorithm, i.e. by letting the gauge links and the electric fields evolve in different steps alternatively. Eqs. (18) and (19) are discretized as

$$U_i(\tau'') = \exp[-2\Delta\tau \cdot iga_\perp E^i(\tau')/\tau'] U_i(\tau), \quad (20)$$

$$U_\eta(\tau'') = \exp[-2\Delta\tau \cdot iga_\eta \tau' E^\eta(\tau')] U_\eta(\tau), \quad (21)$$

where $\tau' = \tau + \Delta\tau/2$ and $\tau'' = \tau + \Delta\tau$. Notice that the exponentiation of the electric field is important, in order to keep the up-to-date gauge links as unitary matrices. In the same fashion, the equations of motion of the electric field are discretized as:

$$E^i(\tau') = E^i(\tau - \Delta\tau) + 2\Delta\tau \frac{i}{2ga_\eta^2 a_\perp \tau} [U_{\eta i}(\tau) + U_{-\eta i}(\tau) - (h.c.)] + 2\Delta\tau \frac{i\tau}{2ga_\perp^3} \sum_{j \neq i} [U_{ji}(\tau) + U_{-ji}(\tau) - (h.c.)],$$

$$E^\eta(\tau') = E^\eta(\tau - \Delta\tau) + 2\Delta\tau \frac{i}{2ga_\eta a_\perp^2 \tau} \sum_{j=x,y} [U_{j\eta}(\tau) + U_{-j\eta}(\tau) - (h.c.)], \quad (22)$$

where

$$U_{\mu\nu}(\mathbf{x}) \equiv U_\mu(\mathbf{x}) U_\nu(\mathbf{x} + \hat{\mu}) U_\mu^\dagger(\mathbf{x} + \hat{\nu}) U_\nu^\dagger(\mathbf{x}) \quad (23)$$

are the plaquette variables. Notice that in this way the gauge links are initialized at time $\tau = 0$, and evolve with integer steps: $\tau = \Delta\tau, 2\Delta\tau, \dots$. Instead, the electric field is initialized at $\tau = \Delta\tau/2$ and proceeds as $\tau = 3\Delta\tau/2, 5\Delta\tau/2, \dots$. Along with the electric fields, using the gauge links we can derive the components of the color-magnetic field as [118]

$$B_x^a = \frac{2}{iga_\eta \tau a_\perp} \text{Tr}[t^a(\mathbb{I} - U_{\eta y})], \quad (24)$$

$$B_y^a = \frac{2}{iga_\eta \tau a_\perp} \text{Tr}[t^a(\mathbb{I} - U_{\eta x})], \quad (25)$$

$$B_z^a = \frac{2}{iga_\perp^2} \text{Tr}[t^a(\mathbb{I} - U_{xy})]. \quad (26)$$

III. HEAVY QUARKS IN THE PRE-EQUILIBRIUM STAGE

In this section, we discuss how we model the diffusion of the heavy quark pairs in the pre-equilibrium stage. Following [104], we model the dynamics of the

quarks in the $c\bar{c}$ and $b\bar{b}$ pairs by semi-classical equations of motion, namely the Wong equations. They describe the time evolution of the coordinate \mathbf{x} , momentum \mathbf{p} , and color charge Q_a , with $a = 1, \dots, N_c^2 - 1$, of the quarks [105, 106]. In the laboratory frame, the Wong

equations read

$$\frac{dx^i}{dt} = \frac{p^i}{E}, \quad (27)$$

$$\frac{dp^i}{dt} = gQ^a F^{i\mu,a} \frac{p_\mu}{E}, \quad (28)$$

$$\frac{dQ^a}{dt} = -g f^{abc} A_\mu^b Q^c \frac{p^\mu}{E}, \quad (29)$$

where $i = x, y, z$ and $\mu = 0, \dots, 3$. Moreover, f^{abc} are the structure constants of the gauge group $SU(N_c)$ and $E = \sqrt{\mathbf{p}^2 + M^2}$ is the kinetic energy of the quark with mass M . The gauge field A_μ is determined by (the A_τ component is zero because of the gauge choice)

$$A_i(\mathbf{x}) = -\left(\frac{i}{ga_\perp}\right) \log U_i(\mathbf{x}), \quad i = x, y, \quad (30)$$

$$A_\eta(\mathbf{x}) = -\left(\frac{i}{ga_\eta}\right) \log U_\eta(\mathbf{x}). \quad (31)$$

whereas the color-electric and color-magnetic fields are defined in terms of the field strength tensor through

$$F_{\tau i} = E_i, \quad F_{\eta i} = \tau \epsilon_{ij} B_j, \quad (32)$$

$$F_{\tau\eta} = \tau E_\eta, \quad F_{xy} = -B_\eta. \quad (33)$$

For $N_c = 3$ the evolution of the color charges governed by Eq. (29) conserves the Casimir invariants

$$q_2 = Q_a Q_a, \quad q_3 = d_{abc} Q_a Q_b Q_c, \quad (34)$$

with

$$q_2 = \frac{N_c^2 - 1}{2} \quad \text{and} \quad q_3 = \frac{(N_c^2 - 4)(N_c^2 - 1)}{4N_c}, \quad (35)$$

and d_{abc} are the symmetric structure constants [77]. The Wong equations have been recently used to study the dynamics of the heavy quarks in the pre-equilibrium stage of high-energy nuclear collisions, see [64–67, 71, 73, 80, 81, 104, 119–121] and references therein. We solve Eqs. (27)–(29) in the background of the evolving glasma fields. Within our model, we follow previous works and neglect the back-reaction of the quarks in the Yang-Mills equations: it has been shown [67] that such back-reaction does not substantially affect the diffusion of heavy quarks within the lifetime of the pre-equilibrium stage.

In this work, following [104] we initialize the quark-antiquark pairs in color-singlet states, as we have in mind the problem of melting of J/ψ and Υ in the pre-equilibrium stage. Despite the initialization in color-singlet states, quarks in this stage are constantly bombarded by the gluons, hence they can exchange color with the gluonic environment and their color charges change. Denoting by Q_a and \bar{Q}_a the color charges of a quark and its antiquark respectively, we consider the

time-dependent quantity

$$\mathcal{G}(\tau) = -\frac{1}{q_2} \text{Tr}(Q_a(\tau) \bar{Q}_b(\tau)) = -\frac{1}{q_2} \sum_a Q_a(\tau) \bar{Q}_a(\tau), \quad (36)$$

where q_2 is the quadratic Casimir invariant of $SU(N_c)$ defined above, and the trace is understood over the (a, b) indices. \mathcal{G} is defined for each of the $c\bar{c}$ and $b\bar{b}$ pairs. For the color-singlet initialization we have $Q_a = -\bar{Q}_a$ at $\tau = \tau_{\text{form}}$, therefore for each pair

$$\mathcal{G} = 1, \quad \tau = \tau_{\text{form}}. \quad (37)$$

We expect that on average the magnitude of \mathcal{G} decreases with time, as a result of the de-correlation of Q_a and \bar{Q}_b due to the random interactions with the gluon fields of the evolving glasma. This decreasing can be interpreted as the raising of the weight of the color-octet component in the pair, which eventually leads to the melting of the pair itself. We will use this idea to define a melting probability of the $c\bar{c}$ and $b\bar{b}$ pairs, see Section V.

As a final remark, we notice that in Eq. (28) we do not add the term describing the static quark-antiquark potential that instead was added in [104]. We do this for simplicity, leaving a complete study to a future work. Although a more realistic calculation should indeed include the terms arising from the color-singlet and the color-octet potentials in the right-hand-side of Eq. (28), it was shown in [104] that when the $c\bar{c}$ and $b\bar{b}$ pairs diffuse in the pre-equilibrium strong gluonic fields, the effect of those is way more important than the effect of the static potentials. For example, it was shown that switching the potential to the color-singlet to the color-octet channel affected the percentage of melted pairs of a few percent only. Consequently, the lack of these potentials in Eq. (28) is not a bad approximation.

IV. HEAVY QUARKS INITIALIZATION

Both $c\bar{c}$ and $b\bar{b}$ quark pairs are produced by hard QCD scatterings between the nucleons of the colliding nuclei at the very early stage of high-energy nuclear collisions, within 0.1 fm/c from the overlap of the two initial nuclei. In this work, we assume the pairs to form at proper time $\tau_{\text{form}} = 1/(2M)$, with M being the heavy-quark mass: $M = 1.3$ GeV for c and $M = 4.2$ GeV for b . Therefore, $\tau_{\text{form}} \sim 0.08$ fm for c , and $\tau_{\text{form}} \sim 0.02$ fm for b .

A. Initialization in the coordinate space

In the transverse plane, the initial positions of the heavy quarks are extracted on an event-by-event basis according to the probability given by the thickness function of the proton, see Eq. (5). For each event, after extracting the position of the three valence quarks via the Gaussian profile (6), HQs positions are extracted via

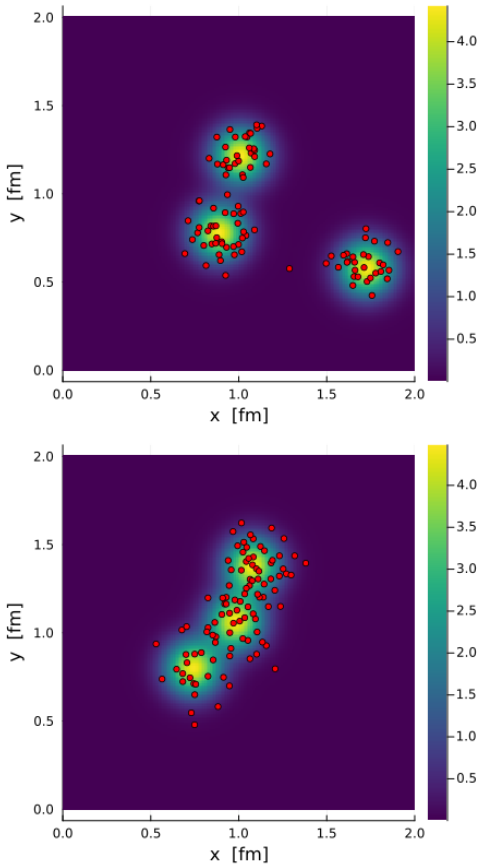


FIG. 1. Production points of the heavy-quark pairs (red dots) on the transverse plane for a proton-nucleus collisions. The background image corresponds to the contour plot of the profile (5), characterized by three hotspots that develop around the valence quarks in that event. We used $g\mu = 1$ GeV for the nucleus. The two panels correspond to two different events.

the profile (5) similarly to what we do for the initialization of the color charges of the proton. In this way, we distribute heavy quarks near the hotspots of the initial energy density of the color fields.

For illustrative purposes, we show in Fig. 1 the position of 100 heavy-quark pairs in two events. We remark that this number of pairs is chosen only for a good visualization and does not correspond to the real number of quarks produced in the considered collision system. In both panels of the figure, the three hotspots correspond to profile (5) that develops around the three valence quarks, the latter location changing event-by-event; we checked that these are the same locations where most of the energy density gets deposited at the initial time. The red dots represent the production points of the heavy-quark pairs. In this work we consider the pairs produced at mid-rapidity, so that the initial longitudinal coordinate of the heavy quarks is $z = 0$, if we indicate with positive z and negative z respectively the forward-going and backward-going directions of the colliding nuclei. For the position of the quark and its antiquark companion in a

pair we have moreover $\mathbf{x}_q = \mathbf{x}_{\bar{q}}$.

B. Initialization in the momentum space

The transverse momenta of the heavy-quark pairs are initialized according to the Fixed Order + Next-to-Leading Log (FONLL) QCD result that reproduces the D -mesons and B -mesons spectra in pp collisions after fragmentation [122–124]. This is achieved by using the following parametrization for the initial transverse momentum spectrum of heavy quarks for collisions at $\sqrt{s_{NN}} = 5.02$ TeV [104]:

$$\left. \frac{dN}{d^2p_T} \right|_{\text{prompt}} = \frac{x_0}{(1 + x_3 \cdot p_T^{x_1})^{x_2}}, \quad (38)$$

with parameters $x_0 = 20.2837$, $x_1 = 1.95061$, $x_2 = 3.13695$, $x_3 = 0.0751663$ for charm quarks and $x_0 = 0.467997$, $x_1 = 1.83805$, $x_2 = 3.07569$, $x_3 = 0.0301554$ for beauty quarks. The azimuthal angle ϕ of each heavy-quark momentum is chosen randomly between 0 and 2π . From ϕ and p_T the components p_x and p_y of the heavy-quark momentum are determined and those of the companion antiquark are fixed as opposite to them. We assume $p_z = 0$ for quarks and their companion antiquarks, as we simulate the mid-rapidity region and assume that the space-time rapidity of the produced particles, $\eta = 0$, is equal to the energy-momentum rapidity, $y = 0$. With this initialization of momenta the quark and antiquark in a pair have momenta, \mathbf{p}_q and $\mathbf{p}_{\bar{q}}$ respectively, such that the total momentum is zero, $\mathbf{p}_q + \mathbf{p}_{\bar{q}} = 0$.

C. Initialization in the color space

Let us deal with the initialization of the color charges appearing in the Wong equations (28) and (29). The initial value of the color charges needs to satisfy the constraints (34). In order to get these, we firstly fix the charge of the first heavy quark in the ensemble to be [77]

$$Q_0^a = -1.69469 \delta^{a5} - 1.06209 \delta^{a8} \quad (39)$$

which explicitly satisfies the conditions (34); then, we generate the charges of all the other heavy quarks as

$$Q^a = Q_0^b U^{ab}, \quad U^{ab} = \frac{1}{T_R} \text{Tr}[T^a U T^b U^\dagger], \quad (40)$$

where $T_R = 1/2$ is such that $\text{Tr}(T^a T^b) = T_R \delta^{ab}$, and U is a random special unitary matrix which is extracted for each heavy quark according to the Haar measure. By construction, all the HQs hereby obtained satisfy (34), and this condition will be satisfied throughout the time evolution, as already stated.

As already anticipated in section III, we initialize the $c\bar{c}$ and $b\bar{b}$ pairs as an ensemble of color-singlet states. By

denoting with Q_a and \bar{Q}_a the color charges of, respectively, the quark and the antiquark in a pair, we impose the condition $Q_a + \bar{Q}_a = 0$. The net color charge carried by each pair therefore vanishes at the formation time.

V. RESULTS

In this section, we show our results on the heavy quark evolution and heavy quark-antiquark pair dissociation in proton-nucleus collisions at LHC energy. Unless differently stated, the results shown in this section have been obtained for a square grid of transverse size $L = 2$ fm, with 32×32 lattice points. In realistic collisions, the pre-equilibrium stage lasts for a fraction of fm/c, but for illustrative purposes, we perform simulations up to 1 fm/c with 1000 time steps (we checked that this number of time steps is enough to have numerical convergence).

A. Momentum broadening

During the propagation in the glasma fields, the heavy quarks undergo a momentum broadening in both the

transverse and longitudinal directions [64–67, 71, 73, 80, 81, 104, 119–121]. This is shown in Fig. 2, where we plot $\delta p_T^2 = \delta p_x^2 + \delta p_y^2$ (purple curves) and δp_z^2 (orange curves), with $\delta p_i^2 = p_i^2(\tau) - p_i^2(\tau_{\text{form}})$, $i = x, y, z$. This quantity describes the amount of momentum accumulated by heavy quarks while they propagate through the medium. Beauty quarks (lower panel) experience a larger momentum broadening than charm ones (upper panel) both in the transverse and longitudinal direction. This can be understood as follows. First of all, charm quarks are produced later and therefore interact with gluon fields that are more diluted (because of the expansion of the system) than those the b quarks interact with. Moreover, the charm quarks initial velocity is higher than that of the beauty quarks, therefore they escape more quickly, with respect to beauty quarks, the regions with intense gluon fields where they are produced.

It is also interesting to note that the longitudinal momentum broadening is larger than the transverse one. This is most likely due to the fact that the longitudinal components of the background gluon fields are stronger than the transverse ones. A semi-quantitative understanding of this fact may be given by studying the momentum broadening of HQs in the limit of infinite mass. As a matter of fact, in this limit we would get [125]

$$\langle \delta p_z^2(\tau) \rangle = g^2 \int_0^\tau d\tau' \int_0^\tau d\tau'' \int d^2 \mathbf{x}_T \langle \text{Tr}[E_z(\tau')E_z(\tau'')] T_p(\mathbf{x}_T) \rangle, \quad (41)$$

$$\langle \delta p_T^2(\tau) \rangle = g^2 \int_0^\tau d\tau' \int_0^\tau d\tau'' \int d^2 \mathbf{x}_T \frac{1}{\tau' \tau''} \text{Tr}([E_x(\tau')E_x(\tau'') + E_y(\tau')E_y(\tau'')] T_p(\mathbf{x}_T)), \quad (42)$$

where T_p is defined in Eq. (5) and takes into account the initial distribution of the HQs in the configuration space. The symbol $\langle \rangle$ in the left hand side of the equations above denotes the ensemble average over the color charges, the average over the transverse plane and a sum over all the HQs, while in the right hand side of the same equations it denotes the ensemble average over the color charges only, as the integration over the whole transverse area is explicit in the equations and the average over the HQs is encoded by the distribution T_p .

In this limit, the transverse momentum broadening is suppressed for large values of the proper time in comparison to the longitudinal one, by a power of $1/\tau^2$. Longitudinal and transverse momentum broadening have been also considered in previous studies, see for example [64–67, 71, 73, 77, 80, 81, 104, 119–121]. In particular, it is interesting to compare our results with those presented in [77], in which the same quantities have been computed in nucleus-nucleus collisions for $N_c = 3$ with an expanding geometry. While the qualitative behavior that we find in pA collisions is similar to that found previously for the case of AA, the momentum broadening for pA is smaller than the one for AA. This quantitative difference is related to the fact that on average the saturation scale of a large nucleus is larger than that of a proton, which results in a energy density in the transverse plane in [77] which is larger with respect to the one we have in our simulations, and consequently in a larger momentum

broadening of the heavy quarks.

B. Spreading of the pairs and color de-correlation

We now focus on heavy quark-antiquark pairs and investigate the effect of the evolving glasma in dissociating the initially produced pairs. The relative position of the quark and antiquark in a pair are modified during their propagation in the fireball, both in the pre-equilibrium and in the thermalized QGP phases. In particular, the interaction with the gluon fields leads to a diffusion in coordinate as well as momentum space, resulting on average in the increase of the relative distance of the two particles in a pair. This is visible in the top panel of Fig. 3, where the relative distance between the quark and its companion antiquark in the rest frame of the pair, r_{rel} , is shown versus the proper time, τ . In the figure, time is

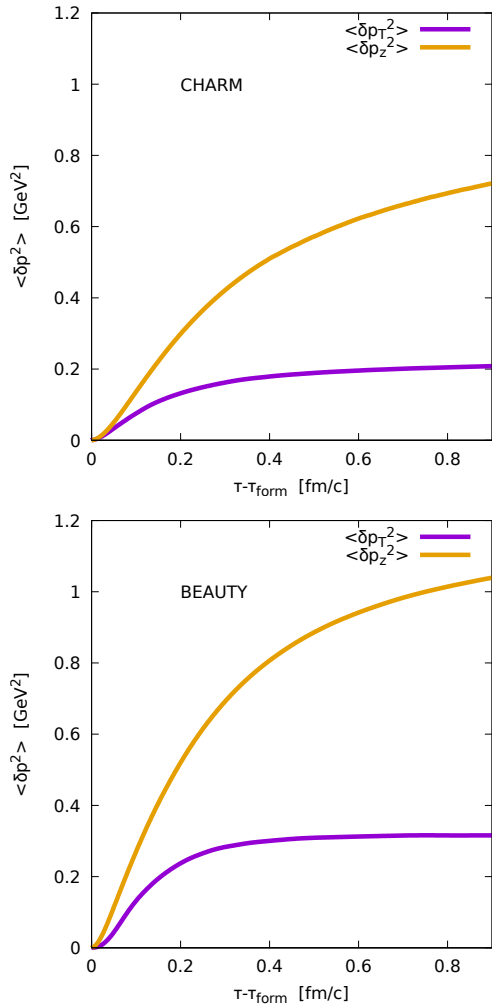


FIG. 2. Momentum broadening of charm (upper panel) and beauty (lower panel) quarks in pA collisions as a function of time $\tau - \tau_{\text{form}}$, with τ_{form} being the heavy-quark formation time. Purple and orange curves correspond to transverse and longitudinal momentum, respectively.

measured with respect to the formation time τ_{form} . Interestingly, We notice that the $c\bar{c}$ system spreads more quickly with respect to the $b\bar{b}$ one as expected, due to the higher masses of b making them more static in the gluon fields.

Not only coordinates and momenta of heavy quarks are affected by the background gluon fields, but also their color charges, see Eq. (29). The quark-antiquark pairs can undergo transitions from singlet to octet (and viceversa) both in glasma and in QGP. In the latter stage, such transitions have been studied especially within the framework of open quantum systems [87, 90, 95]. Singlet-octet transitions may also occur in the glasma stage due to the interaction of the quark and antiquark in the pair with the initial color fields. Though we do not implement the transition to the octet states of the initial color singlet, we consider the de-correlation of the color charges

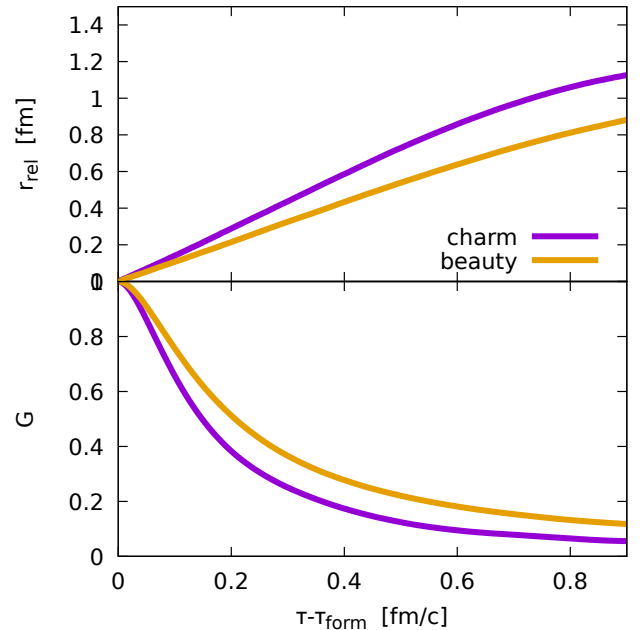


FIG. 3. Relative coordinate (top panel) and color-charge correlator (bottom panel) of the heavy quark-antiquark pair versus time $\tau - \tau_{\text{form}}$, with τ_{form} being the heavy-quark formation time. Purple and orange curves correspond to charm and beauty heavy-quark pairs, respectively.

of the quark and the antiquark in a pair. This quantity serves as an estimate of the probability of singlet-to-octet transitions, and hence gives indications on the survival probability of the pair in the gluon fields.

With the color-singlet initialization that we adopt in this work, the color charges of the two particles in a pair are initially opposite to each other, implying that at $\tau = \tau_{\text{form}}$ the color charges of the quark Q_a and the companion antiquark \bar{Q}_a are maximally anti-correlated. We define the gauge-invariant color-charge correlator [104] as

$$G(\tau) \equiv \langle \mathcal{G}(\tau) \rangle, \quad (43)$$

where \mathcal{G} has been defined in Eq. (36). The brackets in (43) indicate a double average, over the heavy-quark pairs in each events and over the different events corresponding to the ensemble of glasma fields. The correlator (43) satisfies the condition $G(\tau_{\text{form}}) = 1$.

In the lower panel of Fig. 3 we plot $G(\tau)$ versus time $\tau - \tau_{\text{form}}$, for charm (purple line) and beauty (orange line) pairs. We notice that G decreases in time, as expected, indicating a de-correlation of the color charges of the quark and the companion antiquark in a pair. In order to be more quantitative we define a de-correlation time, τ_{dec} , by the requirement that $G(\tau_{\text{dec}}) = 1/2$. We notice that $\tau_{\text{dec}} - \tau_{\text{form}}$ stays in the range (0.2, 0.3) fm/c for both charm and beauty. We also find that $\tau_{\text{dec}} - \tau_{\text{form}}$ for b quarks is slightly larger than the similar quantity computed for the c quarks: this is most likely due to the

fact that b quarks are slower, so they spend more time within correlation domains of the gluonic background. $G(\tau)$ could be interpreted as the probability for pairs to stay in the singlet channel during propagation in the pre-equilibrium stage, or equivalently, $1 - G(\tau)$ as the probability to have singlet-to-octet fluctuations. In fact, at $\tau = \tau_{\text{form}}$ the pairs are in a color-singlet state and the correlator is equal to one; during the evolution, the correlator decreases, that can be interpreted as the fluctuations of the color charges that become gradually more important, making transitions to a color-octet state more probable.

C. Melting of the pairs

We make use of the results discussed in section VB to define a survival probability of the pairs in the pre-equilibrium stage, $\mathcal{P}_{\text{survival}}$, and from this we obtain a melting probability,

$$\mathcal{P}_{\text{melting}} = 1 - \mathcal{P}_{\text{survival}}. \quad (44)$$

In order to define $\mathcal{P}_{\text{survival}}$, it is reasonable to assume that this probability is smaller for larger separation between the quark and its companion antiquark in the pair. Moreover, it is also reasonable to assume that the larger the de-correlation of the color charges in the pair the larger the probability of melting the pair. Therefore, $\mathcal{P}_{\text{survival}}$ can be connected to the quark-antiquark relative position (in the pair rest frame) r_{rel} and \mathcal{G} defined in Eq. (36).

We assume a Gaussian shape of $\mathcal{P}_{\text{survival}}$ in coordinate and color space, namely

$$\mathcal{P}_{\text{survival}} = \mathcal{P}_{\text{distance}} \mathcal{P}_{\text{color}}, \quad (45)$$

where we put

$$\mathcal{P}_{\text{distance}} \equiv \exp\left(-\frac{r_{\text{rel}}^2}{2\sigma_r^2}\right), \quad (46)$$

$$\mathcal{P}_{\text{color}} \equiv \exp(-\kappa(\mathcal{G} - 1)^2), \quad (47)$$

with σ_r and κ being treated as parameters. In particular, σ_r measures the size of the pair, while κ fixes the width of the fluctuations of the color charges that are necessary to break the pair. The form (45) of $\mathcal{P}_{\text{survival}}$ is inspired by the Wigner function of coalescence models to form a vector meson from a quark and an antiquark of the same flavor [111]. The exponent in Eq. (47) takes into account that at $\tau = \tau_{\text{form}}$ we have $\mathcal{G} = 1$, hence the probability that the pair is in the color-singlet state is maximum. In our model, at each time, the status of melted of each quark-antiquark pair is assigned with the probability given by Eq. (44). We notice that in [104] the criterion for pair melting was related only to the average distance of the quark and the antiquark in the pair, while the role of the fluctuations of the color charges was not studied.

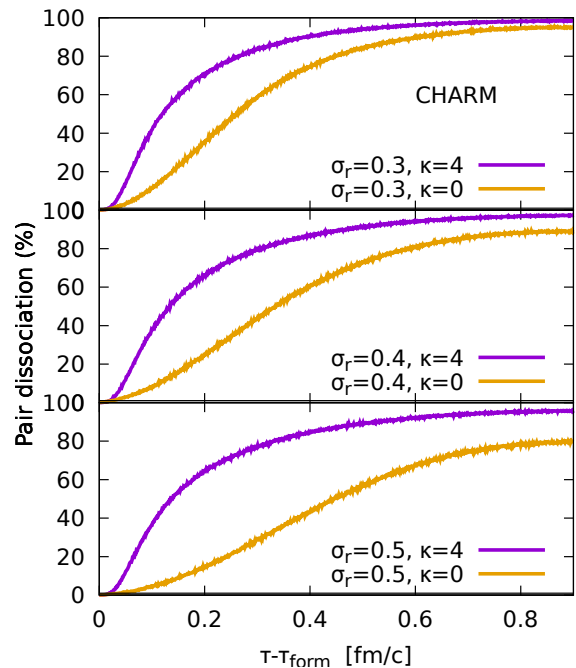


FIG. 4. Percentage of dissociated charm quark-antiquark pairs versus time $\tau - \tau_{\text{form}}$, with τ_{form} being the charm quark formation time. The various curves correspond to different values of the dissociation parameters.

The pairs that survived to the glasma phase may eventually form a bound state and continue propagating in possibly formed QGP medium. The quarks and antiquarks of dissociated pairs may hadronize (after possible evolution in QGP) to form heavy-flavoured hadrons, such as D and B mesons. In this work we consider σ_r and κ as parameters and investigate the effect of glasma on pair dissociation for different values of the two parameters. In particular, we choose $\sigma_r = 0.3, 0.4, 0.5$ fm for charm pairs and $\sigma_r = 0.1, 0.2, 0.3$ fm for beauty pairs. Such values are of the same order of the root mean square radius of charmonium and bottomonium states [126, 127], which represents the spatial extent of their wavefunction. For both flavors we consider two values of the parameter in the color Gaussian, that are $\kappa = 0$ and $\kappa = 4$. In particular, $\kappa = 0$ corresponds to neglecting the effect of color-charge rotation on $\mathcal{P}_{\text{melting}}$ as in [104]. The value $\kappa = 4$ has been chosen so that when $\mathcal{G} = 1/2$ we have $\mathcal{P}_{\text{color}} = 1/e$.

We quantify the impact of the gluon-dominated pre-equilibrium stage of pA collisions on the melting of the pairs by calculating the number of dissociated pair with respect to their initial value. We show this quantity, in percentage, as a function of time $\tau - \tau_{\text{form}}$ in Fig. 4 for $c\bar{c}$ and in Fig. 5 for $b\bar{b}$. The three panels of each figure correspond to different values of the width of the spatial Gaussian. In all panels the orange curves correspond to results obtained with $\kappa = 0$, that is, considering only the effect of distance on pair dissociation; the purple lines

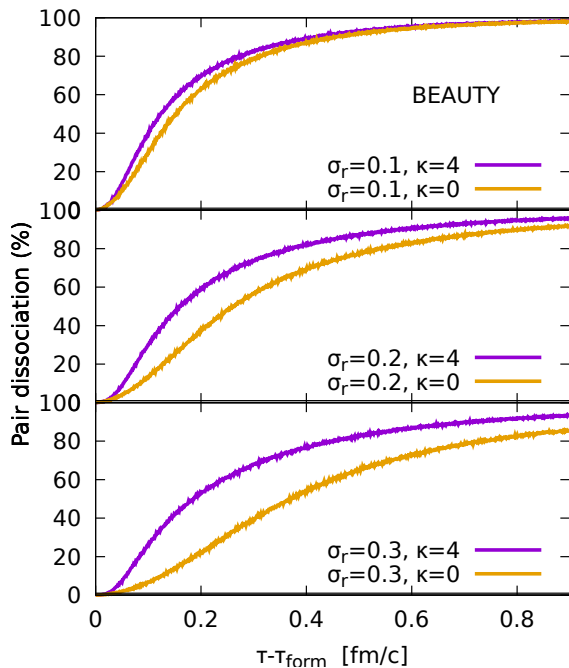


FIG. 5. Percentage of dissociated beauty quark-antiquark pairs versus time $\tau - \tau_{\text{form}}$, with τ_{form} being the beauty quark formation time. The various curves correspond to different values of the dissociation parameters.

are obtained with $\kappa = 4$. Therefore, we can identify the effect of color-charge rotation in color space due to particle interaction with the glasma by comparing the purple with the orange curves. Such effect is larger for charm pairs with respect to the beauty ones; this can be understood by looking at the bottom panel of Fig. 3, where the quicker decay of color-charge correlation for charm quarks is evident. Furthermore, we see a larger difference between the purple and the orange curves for the higher values of σ_r . This is expected because the pair dissociation due to quark-antiquark separation is more probable if a smaller σ_r is considered, indicating a smaller size of the survived pair system.

Introducing the time to break half of the initial pairs, τ_{break} , we found that both for $c\bar{c}$ and for $b\bar{b}$ pairs, $\tau_{\text{break}} - \tau_{\text{form}}$ is around 0.2 fm/c when we consider $\mathcal{P}_{\text{color}}$ in the survival probability, for all the values of σ_r considered. If we ignore the color fluctuations in $\mathcal{P}_{\text{survival}}$, see the orange lines in Figs. 4 and 5, then the melting of the pairs is slower, and $\tau_{\text{break}} - \tau_{\text{form}}$ can even be larger by a factor of 2. Hence, the effect of the interaction of the heavy quarks with the gluon fields in the pre-equilibrium stage is to gradually melt the pairs, due to diffusion in coordinate space, and the color fluctuations accelerate this melting. As a final comment, we notice that our results on the percentage of dissociation and dissociation times are in the same ballpark of those shown in [104] where the melting of pairs in the early stage was studied for the first time, albeit within a simpler model.

VI. CONCLUSIONS

We studied the melting of $c\bar{c}$ and $b\bar{b}$ pairs in the pre-equilibrium stage of high-energy proton-nucleus collisions. We modeled the early stage according to the color-glass-condensate picture, choosing the glasma as the initial condition and solving the classical Yang-Mills equations to study its evolution. The heavy quarks constituting the $c\bar{c}$ and $b\bar{b}$ pairs, which we assume to be produced in color-singlet states, are then evolved on top of the classical gluon fields via semi-classical equations of motion, known as the Wong equations. Our main goal was the calculation of the percentage of pairs that melt during their diffusion in the early stage.

Within our framework, the survival probability of each pair depends on the relative distance of the quark and its companion antiquark, as well as on the fluctuations of the color charges that give a color-octet component to the pair and eventually breaks it. In particular, the color fluctuations are due to the persistent bombardment that the quark and its companion antiquark experience in the dense gluonic bath formed in the early stage. Armed with the survival probability, $\mathcal{P}_{\text{survival}}$, defined in Eq. (45), for each pair at a given time, we accept its survival with probability $\mathcal{P}_{\text{survival}}$. This probability depends on the relative distance as well as on the color charges of the two particles that form the pair: these quantities are directly obtained from the solution of the Wong equations. $\mathcal{P}_{\text{survival}}$ depends on two parameters, which are σ_r that measures the size of the pair, and κ that measures how large the color fluctuations need to be in order to melt the pair.

We studied the evolution of the gauge-invariant correlator of the color charges of the quark and its companion antiquark, $G(\tau)$. At $\tau = \tau_{\text{form}}$ we have $G(\tau_{\text{form}}) = 1$ due to the color-singlet initialization of the pairs. The interaction of the quarks with the dense gluon environment leads to a degradation of the correlations. Consequently, there are fluctuations to the color-octet state at later times, and this process favors the melting of the pairs. The timescale of de-correlation, τ_{dec} , can be estimated, for example, by the requirement that $G(\tau_{\text{dec}}) = 1/2$. We found that $\tau_{\text{dec}} - \tau_{\text{form}}$ stays in the range (0.2, 0.3) fm/c for both charm and beauty. We also find that $\tau_{\text{dec}} - \tau_{\text{form}}$ for b quarks is slightly larger than the similar quantity computed for the c quarks: this is most likely due to the fact that b quarks are slower, so they spend more time within correlation domains of the gluonic background.

Moreover, the diffusion of the heavy quarks in the evolving glasma fields leads to the gradual melting of the pairs. We introduced a breaking time, τ_{break} , defined as the value of the proper time at which half of the pairs melt. We found that for both $c\bar{c}$ and $b\bar{b}$ pairs, $\tau_{\text{break}} - \tau_{\text{form}}$ is around 0.2 fm/c when we include $\mathcal{P}_{\text{color}}$ in the survival probability, for all the values of σ_r considered. Ignoring the color fluctuations in $\mathcal{P}_{\text{survival}}$, the melting of the pairs is slower, and $\tau_{\text{break}} - \tau_{\text{form}}$ can be even twice larger than the time we found when the color

fluctuations are included in the probability.

This work is the natural continuation of [104], in which the same problem has been studied for the $SU(2)$ color group with a static box geometry and for the case of nucleus-nucleus collisions. The most important improvements that we brought, with respect to [104], are the implementation of the expansion of the medium, which takes place both in the longitudinal direction and in the transverse plane; we implemented the $SU(3)$ color group, as well as an initialization engineered for pA collisions that takes into account the event-by-event fluctuations of the color charges in the proton. Finally, we implemented the gauge-invariant formulation in terms of gauge links and plaquettes, while in [104] the authors used the continuum formulation to solve the Yang-Mills equations.

In the study presented here, we neglected the color-singlet and color-octet potentials among the quarks and their companion antiquarks. This simplification is partially justified by the results of [104], in which it was shown that the inclusion of these potentials does not lead to substantial changes in the predictions of the survival probabilities of the pairs. Nevertheless, a complete de-

scription of the dynamics of $c\bar{c}$ and $b\bar{b}$ pairs in the pre-equilibrium stage requires the introduction of those potentials. We plan to include them in future works.

Acknowledgments

The authors acknowledge inspiring discussions with Dana Avramescu and Raju Venugopalan. M. R. acknowledges Bruno Barbieri, Lautaro Martinez and John Petrucci for inspiration. L. O. acknowledges the Next Generation action of the European Commission and the MUR funding (PNRR Missione 4) under the ‘‘Heavy flavour dynamics in the early stage of ultrarelativistic collisions’’ (HEFESTUS) project. This work has been partly funded by the European Union – Next Generation EU through the research grant number P2022Z4P4B ‘‘SOPHYA - Sustainable Optimised PHYSics Algorithms: fundamental physics to build an advanced society’’ under the program PRIN 2022 PNRR of the Italian Ministero dell’Università e Ricerca (MUR).

-
- [1] U. W. Heinz and M. Jacob, Evidence for a new state of matter: An Assessment of the results from the CERN lead beam program, (2000), arXiv:nucl-th/0002042.
- [2] K. Dusling, W. Li, and B. Schenke, Novel collective phenomena in high-energy proton–proton and proton–nucleus collisions, *Int. J. Mod. Phys. E* **25**, 1630002 (2016), arXiv:1509.07939 [nucl-ex].
- [3] M. Greif, C. Greiner, B. Schenke, S. Schlichting, and Z. Xu, Importance of initial and final state effects for azimuthal correlations in p+Pb collisions, *Nucl. Phys. A* **982**, 491 (2019), arXiv:1903.00314 [nucl-th].
- [4] A. Kurkela, U. A. Wiedemann, and B. Wu, Opacity dependence of elliptic flow in kinetic theory, *Eur. Phys. J. C* **79**, 759 (2019), arXiv:1805.04081 [hep-ph].
- [5] A. Kurkela, U. A. Wiedemann, and B. Wu, Flow in AA and pA as an interplay of fluid-like and non-fluid like excitations, *Eur. Phys. J. C* **79**, 965 (2019), arXiv:1905.05139 [hep-ph].
- [6] M. Greif, C. Greiner, B. Schenke, S. Schlichting, and Z. Xu, Importance of initial and final state effects for azimuthal correlations in p+Pb collisions, *Phys. Rev. D* **96**, 091504 (2017), arXiv:1708.02076 [hep-ph].
- [7] W. Zhao, S. Ryu, C. Shen, and B. Schenke, 3D structure of anisotropic flow in small collision systems at energies available at the BNL Relativistic Heavy Ion Collider, *Phys. Rev. C* **107**, 014904 (2023), arXiv:2211.16376 [nucl-th].
- [8] L. Oliva, W. Fan, P. Moreau, S. A. Bass, and E. Bratkovskaya, Nonequilibrium effects and transverse spherocity in ultrarelativistic proton-nucleus collisions, *Phys. Rev. C* **106**, 044910 (2022), arXiv:2204.04194 [nucl-th].
- [9] L. Oliva, W. Fan, P. Moreau, S. A. Bass, and E. Bratkovskaya, Non-equilibrium Dynamics and Collectivity in Ultra-relativistic Proton–Nucleus Collisions, *Acta Phys. Polon. Supp.* **16**, 1 (2023).
- [10] V. Nugara, V. Greco, and S. Plumari, Far-from-equilibrium attractors with Full Relativistic Boltzmann approach in 3+1 D: moments of distribution function and anisotropic flows v_n , (2024), arXiv:2409.12123 [hep-ph].
- [11] J. F. Grosse-Oetringhaus and U. A. Wiedemann, A Decade of Collectivity in Small Systems, (2024), arXiv:2407.07484 [hep-ex].
- [12] T. Lappi and L. McLerran, Some features of the glasma, *Nucl. Phys. A* **772**, 200 (2006), arXiv:hep-ph/0602189.
- [13] L. D. McLerran and R. Venugopalan, Computing quark and gluon distribution functions for very large nuclei, *Phys. Rev. D* **49**, 2233 (1994), arXiv:hep-ph/9309289.
- [14] L. D. McLerran and R. Venugopalan, Gluon distribution functions for very large nuclei at small transverse momentum, *Phys. Rev. D* **49**, 3352 (1994), arXiv:hep-ph/9311205.
- [15] L. D. McLerran and R. Venugopalan, Green’s functions in the color field of a large nucleus, *Phys. Rev. D* **50**, 2225 (1994), arXiv:hep-ph/9402335.
- [16] F. Gelis, E. Iancu, J. Jalilian-Marian, and R. Venugopalan, The Color Glass Condensate, *Ann. Rev. Nucl. Part. Sci.* **60**, 463 (2010), arXiv:1002.0333 [hep-ph].
- [17] E. Iancu and R. Venugopalan, The Color glass condensate and high-energy scattering in QCD, in *Quark-gluon plasma 4*, edited by R. C. Hwa and X.-N. Wang (2003) pp. 249–3363, arXiv:hep-ph/0303204.
- [18] L. McLerran, A Brief Introduction to the Color Glass Condensate and the Glasma, in *38th International Symposium on Multiparticle Dynamics* (2009) pp. 3–18, arXiv:0812.4989 [hep-ph].
- [19] F. Gelis, Color Glass Condensate and Glasma, *Int. J. Mod. Phys. A* **28**, 1330001 (2013), arXiv:1211.3327 [hep-ph].

- [20] B. Schenke, P. Tribedy, and R. Venugopalan, Event-by-event gluon multiplicity, energy density, and eccentricities in ultrarelativistic heavy-ion collisions, *Phys. Rev. C* **86**, 034908 (2012), arXiv:1206.6805 [hep-ph].
- [21] B. Schenke, P. Tribedy, and R. Venugopalan, Fluctuating Glasma initial conditions and flow in heavy ion collisions, *Phys. Rev. Lett.* **108**, 252301 (2012), arXiv:1202.6646 [nucl-th].
- [22] G. D. Moore and D. Teaney, How much do heavy quarks thermalize in a heavy ion collision?, *Phys. Rev. C* **71**, 064904 (2005), arXiv:hep-ph/0412346.
- [23] H. van Hees, V. Greco, and R. Rapp, Heavy-quark probes of the quark-gluon plasma at RHIC, *Phys. Rev. C* **73**, 034913 (2006), arXiv:nucl-th/0508055.
- [24] H. van Hees, M. Mannarelli, V. Greco, and R. Rapp, Nonperturbative heavy-quark diffusion in the quark-gluon plasma, *Phys. Rev. Lett.* **100**, 192301 (2008), arXiv:0709.2884 [hep-ph].
- [25] P. B. Gossiaux and J. Aichelin, Towards an understanding of the RHIC single electron data, *Phys. Rev. C* **78**, 014904 (2008), arXiv:0802.2525 [hep-ph].
- [26] M. He, R. J. Fries, and R. Rapp, Heavy-Quark Diffusion and Hadronization in Quark-Gluon Plasma, *Phys. Rev. C* **86**, 014903 (2012), arXiv:1106.6006 [nucl-th].
- [27] W. M. Alberico, A. Beraudo, A. De Pace, A. Molinari, M. Monteno, M. Nardi, and F. Prino, Heavy-flavour spectra in high energy nucleus-nucleus collisions, *Eur. Phys. J. C* **71**, 1666 (2011), arXiv:1101.6008 [hep-ph].
- [28] T. Lang, H. van Hees, J. Steinheimer, G. Inghirami, and M. Bleicher, Heavy quark transport in heavy ion collisions at energies available at the BNL Relativistic Heavy Ion Collider and at the CERN Large Hadron Collider within the UrQMD hybrid model, *Phys. Rev. C* **93**, 014901 (2016), arXiv:1211.6912 [hep-ph].
- [29] S. K. Das, F. Scardina, S. Plumari, and V. Greco, Heavy-flavor in-medium momentum evolution: Langevin versus Boltzmann approach, *Phys. Rev. C* **90**, 044901 (2014), arXiv:1312.6857 [nucl-th].
- [30] T. Song, H. Berrehrach, D. Cabrera, J. M. Torres-Rincon, L. Tolos, W. Cassing, and E. Bratkovskaya, Tomography of the Quark-Gluon-Plasma by Charm Quarks, *Phys. Rev. C* **92**, 014910 (2015), arXiv:1503.03039 [nucl-th].
- [31] T. Song, H. Berrehrach, D. Cabrera, W. Cassing, and E. Bratkovskaya, Charm production in Pb + Pb collisions at energies available at the CERN Large Hadron Collider, *Phys. Rev. C* **93**, 034906 (2016), arXiv:1512.00891 [nucl-th].
- [32] S. Cao, G.-Y. Qin, and S. A. Bass, Energy loss, hadronization and hadronic interactions of heavy flavors in relativistic heavy-ion collisions, *Phys. Rev. C* **92**, 024907 (2015), arXiv:1505.01413 [nucl-th].
- [33] A. Andronic *et al.*, Heavy-flavour and quarkonium production in the LHC era: from proton-proton to heavy-ion collisions, *Eur. Phys. J. C* **76**, 107 (2016), arXiv:1506.03981 [nucl-ex].
- [34] A. Beraudo, A. De Pace, M. Monteno, M. Nardi, and F. Prino, Heavy-flavour production in high-energy d-Au and p-Pb collisions, *JHEP* **03**, 123, arXiv:1512.05186 [hep-ph].
- [35] S. K. Das, F. Scardina, S. Plumari, and V. Greco, Toward a solution to the R_{AA} and v_2 puzzle for heavy quarks, *Phys. Lett. B* **747**, 260 (2015), arXiv:1502.03757 [nucl-th].
- [36] S. K. Das, M. Ruggieri, S. Mazumder, V. Greco, and J.-e. Alam, Heavy quark diffusion in the pre-equilibrium stage of heavy ion collisions, *J. Phys. G* **42**, 095108 (2015), arXiv:1501.07521 [nucl-th].
- [37] S. K. Das, J. M. Torres-Rincon, L. Tolos, V. Minissale, F. Scardina, and V. Greco, Propagation of heavy baryons in heavy-ion collisions, *Phys. Rev. D* **94**, 114039 (2016), arXiv:1604.05666 [nucl-th].
- [38] S. K. Das, S. Plumari, S. Chatterjee, J. Alam, F. Scardina, and V. Greco, Directed Flow of Charm Quarks as a Witness of the Initial Strong Magnetic Field in Ultra-Relativistic Heavy Ion Collisions, *Phys. Lett. B* **768**, 260 (2017), arXiv:1608.02231 [nucl-th].
- [39] S. Cao, T. Luo, G.-Y. Qin, and X.-N. Wang, Linearized Boltzmann transport model for jet propagation in the quark-gluon plasma: Heavy quark evolution, *Phys. Rev. C* **94**, 014909 (2016), arXiv:1605.06447 [nucl-th].
- [40] G. Aarts *et al.*, Heavy-flavor production and medium properties in high-energy nuclear collisions - What next?, *Eur. Phys. J. A* **53**, 93 (2017), arXiv:1612.08032 [nucl-th].
- [41] F. Prino and R. Rapp, Open Heavy Flavor in QCD Matter and in Nuclear Collisions, *J. Phys. G* **43**, 093002 (2016), arXiv:1603.00529 [nucl-ex].
- [42] F. Scardina, S. K. Das, V. Minissale, S. Plumari, and V. Greco, Estimating the charm quark diffusion coefficient and thermalization time from D meson spectra at energies available at the BNL Relativistic Heavy Ion Collider and the CERN Large Hadron Collider, *Phys. Rev. C* **96**, 044905 (2017), arXiv:1707.05452 [nucl-th].
- [43] S. K. Das, M. Ruggieri, F. Scardina, S. Plumari, and V. Greco, Effect of pre-equilibrium phase on R_{AA} and v_2 of heavy quarks in heavy ion collisions, *J. Phys. G* **44**, 095102 (2017), arXiv:1701.05123 [nucl-th].
- [44] V. Greco, Heavy Flavor Production, Flow and Energy Loss, *Nucl. Phys. A* **967**, 200 (2017).
- [45] Y. Xu, J. E. Bernhard, S. A. Bass, M. Nahrgang, and S. Cao, Data-driven analysis for the temperature and momentum dependence of the heavy-quark diffusion coefficient in relativistic heavy-ion collisions, *Phys. Rev. C* **97**, 014907 (2018), arXiv:1710.00807 [nucl-th].
- [46] S. Chatterjee and P. Bozek, Large directed flow of open charm mesons probes the three dimensional distribution of matter in heavy ion collisions, *Phys. Rev. Lett.* **120**, 192301 (2018), arXiv:1712.01189 [nucl-th].
- [47] S. Chatterjee and P. Bozek, Interplay of drag by hot matter and electromagnetic force on the directed flow of heavy quarks, *Phys. Lett. B* **798**, 134955 (2019), arXiv:1804.04893 [nucl-th].
- [48] A. Beraudo *et al.*, Extraction of Heavy-Flavor Transport Coefficients in QCD Matter, *Nucl. Phys. A* **979**, 21 (2018), arXiv:1803.03824 [nucl-th].
- [49] S. Cao *et al.*, Toward the determination of heavy-quark transport coefficients in quark-gluon plasma, *Phys. Rev. C* **99**, 054907 (2019), arXiv:1809.07894 [nucl-th].
- [50] Y. Xu *et al.*, Resolving discrepancies in the estimation of heavy quark transport coefficients in relativistic heavy-ion collisions, *Phys. Rev. C* **99**, 014902 (2019), arXiv:1809.10734 [nucl-th].
- [51] X. Dong and V. Greco, Heavy quark production and properties of Quark-Gluon Plasma, *Prog. Part. Nucl. Phys.* **104**, 97 (2019).
- [52] T. Song, P. Moreau, J. Aichelin, and E. Bratkovskaya, Exploring non-equilibrium quark-gluon plasma effects

- on charm transport coefficients, *Phys. Rev. C* **101**, 044901 (2020), arXiv:1910.09889 [nucl-th].
- [53] X. Dong, Y.-J. Lee, and R. Rapp, Open Heavy-Flavor Production in Heavy-Ion Collisions, *Ann. Rev. Nucl. Part. Sci.* **69**, 417 (2019), arXiv:1903.07709 [nucl-ex].
- [54] T. Song, P. Moreau, Y. Xu, V. Ozvenchuk, E. Bratkovskaya, J. Aichelin, S. A. Bass, P. B. Gosiaux, and M. Nahrgang, Traces of nonequilibrium effects, initial condition, bulk dynamics, and elementary collisions in the charm observables, *Phys. Rev. C* **101**, 044903 (2020), arXiv:2001.07951 [nucl-th].
- [55] J. Zhao, K. Zhou, S. Chen, and P. Zhuang, Heavy flavors under extreme conditions in high energy nuclear collisions, *Prog. Part. Nucl. Phys.* **114**, 103801 (2020), arXiv:2005.08277 [nucl-th].
- [56] L. Oliva, S. Plumari, and V. Greco, Directed flow of D mesons at RHIC and LHC: non-perturbative dynamics, longitudinal bulk matter asymmetry and electromagnetic fields, *JHEP* **05**, 034, arXiv:2009.11066 [hep-ph].
- [57] L. Oliva, Electromagnetic fields and directed flow in large and small colliding systems at ultrarelativistic energies, *Eur. Phys. J. A* **56**, 255 (2020), arXiv:2007.00560 [nucl-th].
- [58] A. Beraudo, A. De Pace, M. Monteno, M. Nardi, and F. Prino, Rapidity dependence of heavy-flavour production in heavy-ion collisions within a full 3+1 transport approach: quenching, elliptic and directed flow, *JHEP* **05**, 279, arXiv:2102.08064 [hep-ph].
- [59] M. Ruggieri, Pooja, J. Prakash, and S. K. Das, Memory effects on energy loss and diffusion of heavy quarks in the quark-gluon plasma, *Phys. Rev. D* **106**, 034032 (2022), arXiv:2203.06712 [hep-ph].
- [60] Pooja, S. K. Das, V. Greco, and M. Ruggieri, Thermalization and isotropization of heavy quarks in a non-Markovian medium in high-energy nuclear collisions, *Phys. Rev. D* **108**, 054026 (2023), arXiv:2306.13749 [hep-ph].
- [61] Y. Sun, S. Plumari, and S. K. Das, Exploring the effects of electromagnetic fields and tilted bulk distribution on directed flow of D mesons in small systems, *Phys. Lett. B* **843**, 138043 (2023), arXiv:2304.12792 [nucl-th].
- [62] S. K. Das, J. M. Torres-Rincon, and R. Rapp, Charm and Bottom Hadrons in Hot Hadronic Matter, (2024), arXiv:2406.13286 [hep-ph].
- [63] S. Mrowczynski, Heavy Quarks in Turbulent QCD Plasmas, *Eur. Phys. J. A* **54**, 43 (2018), arXiv:1706.03127 [nucl-th].
- [64] M. Ruggieri and S. K. Das, Cathode tube effect: Heavy quarks probing the glasma in p-Pb collisions, *Phys. Rev. D* **98**, 094024 (2018), arXiv:1805.09617 [nucl-th].
- [65] Y. Sun, G. Coci, S. K. Das, S. Plumari, M. Ruggieri, and V. Greco, Impact of Glasma on heavy quark observables in nucleus-nucleus collisions at LHC, *Phys. Lett. B* **798**, 134933 (2019), arXiv:1902.06254 [nucl-th].
- [66] J. H. Liu, S. Plumari, S. K. Das, V. Greco, and M. Ruggieri, Diffusion of heavy quarks in the early stage of high-energy nuclear collisions at energies available at the BNL Relativistic Heavy Ion Collider and at the CERN Large Hadron Collider, *Phys. Rev. C* **102**, 044902 (2020), arXiv:1911.02480 [nucl-th].
- [67] J.-H. Liu, S. K. Das, V. Greco, and M. Ruggieri, Ballistic diffusion of heavy quarks in the early stage of relativistic heavy ion collisions at RHIC and the LHC, *Phys. Rev. D* **103**, 034029 (2021), arXiv:2011.05818 [hep-ph].
- [68] K. Boguslavski, A. Kurkela, T. Lappi, and J. Peuron, Heavy quark diffusion in an overoccupied gluon plasma, *JHEP* **09**, 077, arXiv:2005.02418 [hep-ph].
- [69] M. E. Carrington, A. Czajka, and S. Mrowczynski, Heavy Quarks Embedded in Glasma, *Nucl. Phys. A* **1001**, 121914 (2020), arXiv:2001.05074 [nucl-th].
- [70] A. Ipp, D. I. Müller, and D. Schuh, Jet momentum broadening in the pre-equilibrium Glasma, *Phys. Lett. B* **810**, 135810 (2020), arXiv:2009.14206 [hep-ph].
- [71] P. Khowal, S. K. Das, L. Oliva, and M. Ruggieri, Heavy quarks in the early stage of high energy nuclear collisions at RHIC and LHC: Brownian motion versus diffusion in the evolving Glasma, *Eur. Phys. J. Plus* **137**, 307 (2022), arXiv:2110.14610 [hep-ph].
- [72] M. E. Carrington, A. Czajka, and S. Mrowczynski, Jet quenching in glasma, *Phys. Lett. B* **834**, 137464 (2022), arXiv:2112.06812 [hep-ph].
- [73] Pooja, S. K. Das, V. Greco, and M. Ruggieri, Anisotropic fluctuations of angular momentum of heavy quarks in the Glasma, *Eur. Phys. J. Plus* **138**, 313 (2023), arXiv:2212.09725 [hep-ph].
- [74] M. E. Carrington, A. Czajka, and S. Mrowczynski, Transport of hard probes through glasma, *Phys. Rev. C* **105**, 064910 (2022), arXiv:2202.00357 [nucl-th].
- [75] S. K. Das *et al.*, Dynamics of Hot QCD Matter – Current Status and Developments, *Int. J. Mod. Phys. E* **31**, 12 (2022), arXiv:2208.13440 [nucl-th].
- [76] K. Boguslavski, A. Kurkela, T. Lappi, F. Lindenbauer, and J. Peuron, Heavy quark diffusion coefficient in heavy-ion collisions via kinetic theory, *Phys. Rev. D* **109**, 014025 (2024), arXiv:2303.12520 [hep-ph].
- [77] D. Avramescu, V. Băran, V. Greco, A. Ipp, D. I. Müller, and M. Ruggieri, Simulating jets and heavy quarks in the glasma using the colored particle-in-cell method, *Phys. Rev. D* **107**, 114021 (2023), arXiv:2303.05599 [hep-ph].
- [78] H. Pandey, S. Schlichting, and S. Sharma, Heavy-Quark Momentum Broadening in a Non-Abelian Plasma away from Thermal Equilibrium, *Phys. Rev. Lett.* **132**, 222301 (2024), arXiv:2312.12280 [hep-lat].
- [79] K. Boguslavski, A. Kurkela, T. Lappi, F. Lindenbauer, and J. Peuron, Jet momentum broadening during initial stages in heavy-ion collisions, *Phys. Lett. B* **850**, 138525 (2024), arXiv:2303.12595 [hep-ph].
- [80] D. Avramescu, V. Greco, T. Lappi, H. Mäntysaari, and D. Müller, The impact of glasma on heavy flavor azimuthal correlations and spectra, (2024), arXiv:2409.10564 [hep-ph].
- [81] D. Avramescu, V. Greco, T. Lappi, H. Mäntysaari, and D. Müller, Heavy flavor angular correlations as a direct probe of the glasma, (2024), arXiv:2409.10565 [hep-ph].
- [82] T. Matsui and H. Satz, J/ψ Suppression by Quark-Gluon Plasma Formation, *Phys. Lett. B* **178**, 416 (1986).
- [83] S. Datta, F. Karsch, P. Petreczky, and I. Wetzorke, Behavior of charmonium systems after deconfinement, *Phys. Rev. D* **69**, 094507 (2004), arXiv:hep-lat/0312037.
- [84] Y. Burnier, M. Laine, and M. Vepsäläinen, Quarkonium dissociation in the presence of a small momentum space anisotropy, *Phys. Lett. B* **678**, 86 (2009), arXiv:0903.3467 [hep-ph].
- [85] N. Brambilla, M. A. Escobedo, J. Ghiglieri, and A. Vairo, Thermal width and gluo-dissociation of quarkonium in pNRQCD, *JHEP* **12**, 116,

- arXiv:1109.5826 [hep-ph].
- [86] P. K. Srivastava, M. Mishra, and C. P. Singh, Color screening scenario for quarkonia suppression in a quasi-particle model compared with data obtained from experiments at the CERN SPS, BNL RHIC, and CERN LHC, *Phys. Rev. C* **87**, 034903 (2013), arXiv:1208.4796 [hep-ph].
- [87] J. Casalderrey-Solana, Dynamical Quarkonia Suppression in a QGP-Brick, *JHEP* **03**, 091, arXiv:1208.2602 [hep-ph].
- [88] N. Brambilla, M. A. Escobedo, J. Ghiglieri, and A. Vairo, Thermal width and quarkonium dissociation by inelastic parton scattering, *JHEP* **05**, 130, arXiv:1303.6097 [hep-ph].
- [89] C. R. Singh, P. K. Srivastava, S. Ganesh, and M. Mishra, Unified description of charmonium suppression in a quark-gluon plasma medium at RHIC and LHC energies, *Phys. Rev. C* **92**, 034916 (2015), arXiv:1505.05674 [hep-ph].
- [90] N. Brambilla, M. A. Escobedo, J. Soto, and A. Vairo, Quarkonium suppression in heavy-ion collisions: an open quantum system approach, *Phys. Rev. D* **96**, 034021 (2017), arXiv:1612.07248 [hep-ph].
- [91] T. Song, J. Aichelin, and E. Bratkovskaya, Production of primordial J/ψ in relativistic $p+p$ and heavy-ion collisions, *Phys. Rev. C* **96**, 014907 (2017), arXiv:1705.00046 [nucl-th].
- [92] Y. Akamatsu, Quarkonium in quark-gluon plasma: Open quantum system approaches re-examined, *Prog. Part. Nucl. Phys.* **123**, 103932 (2022), arXiv:2009.10559 [nucl-th].
- [93] X. Yao, Open quantum systems for quarkonia, *Int. J. Mod. Phys. A* **36**, 2130010 (2021), arXiv:2102.01736 [hep-ph].
- [94] M. He, B. Wu, and R. Rapp, Collectivity of J/ψ Mesons in Heavy-Ion Collisions, *Phys. Rev. Lett.* **128**, 162301 (2022), arXiv:2111.13528 [nucl-th].
- [95] T. Miura, Y. Akamatsu, M. Asakawa, and Y. Kaida, Simulation of Lindblad equations for quarkonium in the quark-gluon plasma, *Phys. Rev. D* **106**, 074001 (2022), arXiv:2205.15551 [nucl-th].
- [96] D. Y. A. Villar, J. Zhao, J. Aichelin, and P. B. Gossiaux, New microscopic model for J/ψ production in heavy ion collisions, *Phys. Rev. C* **107**, 054913 (2023), arXiv:2206.01308 [nucl-th].
- [97] N. Brambilla, M. A. Escobedo, A. Islam, M. Strickland, A. Tiwari, A. Vairo, and P. Vander Griend, Heavy quarkonium dynamics at next-to-leading order in the binding energy over temperature, *JHEP* **08**, 303, arXiv:2205.10289 [hep-ph].
- [98] T. Song, J. Aichelin, J. Zhao, P. B. Gossiaux, and E. Bratkovskaya, Bottomonium production in pp and heavy-ion collisions, *Phys. Rev. C* **108**, 054908 (2023), arXiv:2305.10750 [nucl-th].
- [99] T. Song, J. Aichelin, and E. Bratkovskaya, Charmonium production in a thermalizing heat bath, *Phys. Rev. C* **107**, 054906 (2023), arXiv:2302.14001 [hep-ph].
- [100] N. Brambilla, T. Magorsch, M. Strickland, A. Vairo, and P. Vander Griend, Bottomonium suppression from the three-loop QCD potential, *Phys. Rev. D* **109**, 114016 (2024), arXiv:2403.15545 [hep-ph].
- [101] A. Andronic *et al.*, Comparative study of quarkonium transport in hot QCD matter, *Eur. Phys. J. A* **60**, 88 (2024), arXiv:2402.04366 [nucl-th].
- [102] Y. Bai and B. Chen, Probing QGP droplets with charmonium in high-multiplicity proton-proton collisions, *Eur. Phys. J. C* **84**, 1193 (2024), arXiv:2407.10566 [nucl-th].
- [103] A. Rothkopf, Heavy Quarkonium in Extreme Conditions, *Phys. Rept.* **858**, 1 (2020), arXiv:1912.02253 [hep-ph].
- [104] Pooja, M. Y. Jamal, P. P. Bhaduri, M. Ruggieri, and S. K. Das, cc^- and bb^- suppression in the glasma, *Phys. Rev. D* **110**, 094018 (2024), arXiv:2404.05315 [hep-ph].
- [105] S. K. Wong, Field and particle equations for the classical Yang-Mills field and particles with isotopic spin, *Nuovo Cim. A* **65**, 689 (1970).
- [106] U. W. Heinz, Quark - Gluon Transport Theory. Part 1. the Classical Theory, *Annals Phys.* **161**, 48 (1985).
- [107] V. Greco, C. M. Ko, and P. Levai, Parton coalescence and anti-proton / pion anomaly at RHIC, *Phys. Rev. Lett.* **90**, 202302 (2003), arXiv:nucl-th/0301093.
- [108] R. J. Fries, B. Muller, C. Nonaka, and S. A. Bass, Hadronization in heavy ion collisions: Recombination and fragmentation of partons, *Phys. Rev. Lett.* **90**, 202303 (2003), arXiv:nucl-th/0301087.
- [109] V. Greco, C. M. Ko, and P. Levai, Parton coalescence at RHIC, *Phys. Rev. C* **68**, 034904 (2003), arXiv:nucl-th/0305024.
- [110] R. J. Fries, B. Muller, C. Nonaka, and S. A. Bass, Hadron production in heavy ion collisions: Fragmentation and recombination from a dense parton phase, *Phys. Rev. C* **68**, 044902 (2003), arXiv:nucl-th/0306027.
- [111] V. Greco, C. M. Ko, and R. Rapp, Quark coalescence for charmed mesons in ultrarelativistic heavy ion collisions, *Phys. Lett. B* **595**, 202 (2004), arXiv:nucl-th/0312100.
- [112] S. Plumari, V. Minissale, S. K. Das, G. Coci, and V. Greco, Charmed Hadrons from Coalescence plus Fragmentation in relativistic nucleus-nucleus collisions at RHIC and LHC, *Eur. Phys. J. C* **78**, 348 (2018), arXiv:1712.00730 [hep-ph].
- [113] T. Lappi, Small x physics and RHIC data, *Int. J. Mod. Phys. E* **20**, 1 (2011), arXiv:1003.1852 [hep-ph].
- [114] B. Schenke, C. Shen, and P. Tribedy, Running the gamut of high energy nuclear collisions, *Phys. Rev. C* **102**, 044905 (2020), arXiv:2005.14682 [nucl-th].
- [115] A. H. Rezaeian, M. Siddikov, M. Van de Klundert, and R. Venugopalan, Analysis of combined HERA data in the Impact-Parameter dependent Saturation model, *Phys. Rev. D* **87**, 034002 (2013), arXiv:1212.2974 [hep-ph].
- [116] C.-N. Yang and R. L. Mills, Conservation of Isotopic Spin and Isotopic Gauge Invariance, *Phys. Rev.* **96**, 191 (1954).
- [117] A. Krasnitz and R. Venugopalan, Nonperturbative computation of gluon minijet production in nuclear collisions at very high-energies, *Nucl. Phys. B* **557**, 237 (1999), arXiv:hep-ph/9809433.
- [118] K. Fukushima and F. Gelis, The evolving Glasma, *Nucl. Phys. A* **874**, 108 (2012), arXiv:1106.1396 [hep-ph].
- [119] M. Ruggieri and S. K. Das, Diffusion of charm and beauty in the Glasma, *EPJ Web Conf.* **192**, 00017 (2018), arXiv:1809.07915 [nucl-th].
- [120] M. Y. Jamal, S. K. Das, and M. Ruggieri, Energy Loss Versus Energy Gain of Heavy Quarks in a Hot Medium, *Phys. Rev. D* **103**, 054030 (2021), arXiv:2009.00561 [nucl-th].

- [121] Y. Sun, G. Coci, S. K. Das, S. Plumari, M. Ruggieri, and V. Greco, Impact of Glasma on heavy quark R_{AA} and v_2 in nucleus-nucleus collisions at LHC, Nucl. Phys. A **1005**, 121913 (2021).
- [122] M. Cacciari, M. Greco, and P. Nason, The p_T spectrum in heavy-flavour hadroproduction., JHEP **05**, 007, arXiv:hep-ph/9803400.
- [123] M. Cacciari, S. Frixione, and P. Nason, The p(T) spectrum in heavy flavor photoproduction, JHEP **03**, 006, arXiv:hep-ph/0102134.
- [124] M. Cacciari, S. Frixione, N. Houdeau, M. L. Mangano, P. Nason, and G. Ridolfi, Theoretical predictions for charm and bottom production at the LHC, JHEP **10**, 137, arXiv:1205.6344 [hep-ph].
- [125] G. Parisi, V. Greco, and M. Ruggieri, in preparation, .
- [126] D. Ebert, R. N. Faustov, and V. O. Galkin, Spectroscopy and Regge trajectories of heavy quarkonia and B_c mesons, Eur. Phys. J. C **71**, 1825 (2011), arXiv:1111.0454 [hep-ph].
- [127] E. Omugbe, E. P. Inyang, I. J. Njoku, C. Martínez-Flores, A. Jahanshir, I. B. Okon, E. S. Eyube, R. Horchani, and C. A. Onate, Approximate mass spectra and root mean square radii of quarkonia using Cornell potential plus spin-spin interactions, Nucl. Phys. A **1034**, 122653 (2023).